

Suppression of Back-to-Back Hadron Pairs at Forward Rapidity in $d + \text{Au}$ Collisions at $\sqrt{s_{NN}} = 200 \text{ GeV}$

A. Adare,¹¹ S. Afanasiev,²⁶ C. Aidala,³⁹ N. N. Ajitanand,⁵⁵ Y. Akiba,^{50,51} H. Al-Bataineh,⁴⁵ J. Alexander,⁵⁵ A. Angerami,¹² K. Aoki,^{32,50} N. Apadula,⁵⁶ Y. Aramaki,¹⁰ E. T. Atomssa,³³ R. Averbeck,⁵⁶ T. C. Awes,⁴⁶ B. Azmoun,⁵ V. Babintsev,²¹ M. Bai,⁴ G. Baksay,¹⁷ L. Baksay,¹⁷ K. N. Barish,⁶ B. Bassalleck,⁴⁴ A. T. Basye,¹ S. Bathe,^{6,51} V. Baublis,⁴⁹ C. Baumann,⁴⁰ A. Bazilevsky,⁵ S. Belikov,^{5,*} R. Belmont,⁶⁰ R. Bennett,⁵⁶ A. Berdnikov,⁵³ Y. Berdnikov,⁵³ J. H. Bhom,⁶³ D. S. Blau,³¹ J. S. Bok,⁶³ K. Boyle,⁵⁶ M. L. Brooks,³⁵ H. Buesching,⁵ V. Bumazhnov,²¹ G. Bunce,^{5,51} S. Butsyk,³⁵ S. Campbell,⁵⁶ A. Caringi,⁴¹ C.-H. Chen,⁵⁶ C. Y. Chi,¹² M. Chiu,⁵ I. J. Choi,⁶³ J. B. Choi,⁸ R. K. Choudhury,³ P. Christiansen,³⁷ T. Chujo,⁵⁹ P. Chung,⁵⁵ O. Chvala,⁶ V. Cianciolo,⁴⁶ Z. Citron,⁵⁶ B. A. Cole,¹² Z. Conesa del Valle,³³ M. Connors,⁵⁶ M. Csanád,¹⁵ T. Csörgő,²⁹ T. Dahms,⁵⁶ S. Dairaku,^{32,50} I. Danchev,⁶⁰ K. Das,¹⁸ A. Datta,³⁹ G. David,⁵ M. K. Dayananda,¹⁹ A. Denisov,²¹ A. Deshpande,^{51,56} E. J. Desmond,⁵ K. V. Dharmawardane,⁴⁵ O. Dietzsch,⁵⁴ A. Dion,²⁵ M. Donadelli,⁵⁴ O. Drapier,³³ A. Drees,⁵⁶ K. A. Drees,⁴ J. M. Durham,⁵⁶ A. Durum,²¹ D. Dutta,³ L. D'Orazio,³⁸ S. Edwards,¹⁸ Y. V. Efremenko,⁴⁶ F. Ellinghaus,¹¹ T. Engelmöre,¹² A. Enokizono,⁴⁶ H. En'yo,^{50,51} S. Esumi,⁵⁹ B. Fadem,⁴¹ D. E. Fields,⁴⁴ M. Finger,⁷ M. Finger, Jr.,⁷ F. Fleuret,³³ S. L. Fokin,³¹ Z. Fraenkel,^{62,*} J. E. Frantz,⁵⁶ A. Franz,⁵ A. D. Frawley,¹⁸ K. Fujiwara,⁵⁰ Y. Fukao,⁵⁰ T. Fusayasu,⁴³ I. Garishvili,⁵⁷ A. Glenn,³⁴ H. Gong,⁵⁶ M. Gonin,³³ Y. Goto,^{50,51} R. Granier de Cassagnac,³³ N. Grau,¹² S. V. Greene,⁶⁰ G. Grim,³⁵ M. Grosse Perdekamp,²² T. Gunji,¹⁰ H.-Å. Gustafsson,^{37,*} J. S. Haggerty,⁵ K. I. Hahn,¹⁶ H. Hamagaki,¹⁰ J. Hamblen,⁵⁷ R. Han,⁴⁸ J. Hanks,¹² E. Haslum,³⁷ R. Hayano,¹⁰ X. He,¹⁹ M. Heffner,³⁴ T. K. Hemmick,⁵⁶ T. Hester,⁶ J. C. Hill,²⁵ M. Hohlmann,¹⁷ W. Holzmann,¹² K. Homma,²⁰ B. Hong,³⁰ T. Horaguchi,²⁰ D. Hornback,⁵⁷ S. Huang,⁶⁰ T. Ichihara,^{50,51} R. Ichimiya,⁵⁰ Y. Ikeda,⁵⁹ K. Imai,^{32,50} M. Inaba,⁵⁹ D. Isenhower,¹ M. Ishihara,⁵⁰ M. Issah,⁶⁰ A. Isupov,²⁶ D. Ivanischev,⁴⁹ Y. Iwanaga,²⁰ B. V. Jacak,^{56,†} J. Jia,^{5,55} X. Jiang,³⁵ J. Jin,¹² B. M. Johnson,⁵ T. Jones,¹ K. S. Joo,⁴² D. Jouan,⁴⁷ D. S. Jumper,¹ F. Kajihara,¹⁰ J. Kamin,⁵⁶ J. H. Kang,⁶³ J. Kapustinsky,³⁵ K. Karatsu,³² M. Kasai,^{52,50} D. Kallow,^{39,51} M. Kawashima,^{52,50} A. V. Kazantsev,³¹ T. Kempel,²⁵ A. Khanzadeev,⁴⁹ K. M. Kijima,²⁰ J. Kikuchi,⁶¹ A. Kim,¹⁶ B. I. Kim,³⁰ D. J. Kim,²⁷ E. J. Kim,⁸ Y.-J. Kim,²² E. Kinney,¹¹ Á. Kiss,¹⁵ E. Kistenev,⁵ L. Kochenda,⁴⁹ B. Komkov,⁴⁹ M. Konno,⁵⁹ J. Koster,²² A. Král,¹³ A. Kravitz,¹² G. J. Kunde,³⁵ K. Kurita,^{52,50} M. Kurosawa,⁵⁰ Y. Kwon,⁶³ G. S. Kyle,⁴⁵ R. Lacey,⁵⁵ Y. S. Lai,¹² J. G. Lajoie,²⁵ A. Lebedev,²⁵ D. M. Lee,³⁵ J. Lee,¹⁶ K. B. Lee,³⁰ K. S. Lee,³⁰ M. J. Leitch,³⁵ M. A. L. Leite,⁵⁴ X. Li,⁹ P. Lichtenwalner,⁴¹ P. Liebing,⁵¹ L. A. Linden Levy,¹¹ T. Liška,¹³ A. Litvinenko,²⁶ H. Liu,³⁵ M. X. Liu,³⁵ B. Love,⁶⁰ D. Lynch,⁵ C. F. Maguire,⁶⁰ Y. I. Makdisi,⁴ A. Malakhov,²⁶ M. D. Malik,⁴⁴ V. I. Manko,³¹ E. Mannel,¹² Y. Mao,^{48,50} H. Masui,⁵⁹ F. Matathias,¹² M. McCumber,⁵⁶ P. L. McGaughey,³⁵ N. Means,⁵⁶ B. Meredith,²² Y. Miake,⁵⁹ T. Mibe,²⁸ A. C. Mignerey,³⁸ K. Miki,^{50,59} A. Milov,⁵ J. T. Mitchell,⁵ A. K. Mohanty,³ H. J. Moon,⁴² Y. Morino,¹⁰ A. Morreale,⁶ D. P. Morrison,⁵ T. V. Moukhanova,³¹ T. Murakami,³² J. Murata,^{52,50} S. Nagamiya,²⁸ J. L. Nagle,¹¹ M. Naglis,⁶² M. I. Nagy,²⁹ I. Nakagawa,^{50,51} Y. Nakamiya,²⁰ K. R. Nakamura,³² T. Nakamura,⁵⁰ K. Nakano,⁵⁰ S. Nam,¹⁶ J. Newby,³⁴ M. Nguyen,⁵⁶ M. Nihashi,²⁰ R. Nouicer,⁵ A. S. Nyanin,³¹ C. Oakley,¹⁹ E. O'Brien,⁵ S. X. Oda,¹⁰ C. A. Ogilvie,²⁵ M. Oka,⁵⁹ K. Okada,⁵¹ Y. Onuki,⁵⁰ A. Oskarsson,³⁷ M. Ouchida,^{20,50} K. Ozawa,¹⁰ R. Pak,⁵ V. Pantuev,^{23,56} V. Papavassiliou,⁴⁵ I. H. Park,¹⁶ S. K. Park,³⁰ W. J. Park,³⁰ S. F. Pate,⁴⁵ H. Pei,²⁵ J.-C. Peng,²² H. Pereira,¹⁴ V. Peresedov,²⁶ D. Yu. Peressoukko,³¹ R. Petti,⁵⁶ C. Pinkenburg,⁵ R. P. Pisani,⁵ M. Proissl,⁵⁶ M. L. Purschke,⁵ H. Qu,¹⁹ J. Rak,²⁷ I. Ravinovich,⁶² K. F. Read,^{46,57} K. Reygers,⁴⁰ V. Riabov,⁴⁹ Y. Riabov,⁴⁹ E. Richardson,³⁸ D. Roach,⁶⁰ G. Roche,³⁶ S. D. Rolnick,⁶ M. Rosati,²⁵ C. A. Rosen,¹¹ S. S. E. Rosendahl,³⁷ P. Rukoyatkin,²⁶ P. Ružička,²⁴ B. Sahlmueller,⁴⁰ N. Saito,²⁸ T. Sakaguchi,⁵ K. Sakashita,^{50,58} V. Samsonov,⁴⁹ S. Sano,^{10,61} T. Sato,⁵⁹ S. Sawada,²⁸ K. Sedgwick,⁶ J. Seele,¹¹ R. Seidl,^{22,51} R. Seto,⁶ D. Sharma,⁶² I. Shein,²¹ T.-A. Shibata,^{50,58} K. Shigaki,²⁰ M. Shimomura,⁵⁹ K. Shoji,^{32,50} P. Shukla,³ A. Sickles,⁵ C. L. Silva,²⁵ D. Silvermyr,⁴⁶ C. Silvestre,¹⁴ K. S. Sim,³⁰ B. K. Singh,² C. P. Singh,² V. Singh,² M. Slunečka,⁷ R. A. Soltz,³⁴ W. E. Sondheim,³⁵ S. P. Sorensen,⁵⁷ I. V. Sourikova,⁵ P. W. Stankus,⁴⁶ E. Stenlund,³⁷ S. P. Stoll,⁵ T. Sugitate,²⁰ A. Sukhanov,⁵ J. Sziklai,²⁹ E. M. Takagui,⁵⁴ A. Taketani,^{50,51} R. Tanabe,⁵⁹ Y. Tanaka,⁴³ S. Taneja,⁵⁶ K. Tanida,^{32,50,51} M. J. Tannenbaum,⁵ S. Tarafdar,² A. Taranenko,⁵⁵ H. Themann,⁵⁶ D. Thomas,¹ T. L. Thomas,⁴⁴ M. Togawa,⁵¹ A. Toia,⁵⁶ L. Tomášek,²⁴ H. Torii,²⁰ R. S. Towell,¹ I. Tseruya,⁶² Y. Tsuchimoto,²⁰ C. Vale,⁵ H. Valle,⁶⁰ H. W. van Hecke,³⁵ E. Vazquez-Zambrano,¹² A. Veicht,²² J. Velkovska,⁶⁰ R. Vértési,²⁹ M. Virius,¹³ V. Vrba,²⁴ E. Vznuzdaev,⁴⁹ X. R. Wang,⁴⁵ D. Watanabe,²⁰ K. Watanabe,⁵⁹ Y. Watanabe,^{50,51} F. Wei,²⁵ R. Wei,⁵⁵ J. Wessels,⁴⁰ S. N. White,⁵ D. Winter,¹² C. L. Woody,⁵ R. M. Wright,¹ M. Wysocki,¹¹ Y. L. Yamaguchi,¹⁰ K. Yamaura,²⁰ R. Yang,²²

A. Yanovich,²¹ J. Ying,¹⁹ S. Yokkaichi,^{50,51} Z. You,⁴⁸ G. R. Young,⁴⁶ I. Younus,⁴⁴ I. E. Yushmanov,³¹
W. A. Zajc,¹² S. Zhou,⁹ and L. Zolin²⁶

(PHENIX Collaboration)

¹Abilene Christian University, Abilene, Texas 79699, USA

²Department of Physics, Banaras Hindu University, Varanasi 221005, India

³Bhabha Atomic Research Centre, Bombay 400 085, India

⁴Collider-Accelerator Department, Brookhaven National Laboratory, Upton, New York 11973-5000, USA

⁵Physics Department, Brookhaven National Laboratory, Upton, New York 11973-5000, USA

⁶University of California-Riverside, Riverside, California 92521, USA

⁷Charles University, Ovocný trh 5, Praha 1, 116 36, Prague, Czech Republic

⁸Chonbuk National University, Jeonju, 561-756, Korea

⁹China Institute of Atomic Energy (CIAE), Beijing, People's Republic of China

¹⁰Center for Nuclear Study, Graduate School of Science, University of Tokyo, 7-3-1 Hongo, Bunkyo, Tokyo 113-0033, Japan

¹¹University of Colorado, Boulder, Colorado 80309, USA

¹²Columbia University, New York, New York 10027 and Nevis Laboratories, Irvington, New York 10533, USA

¹³Czech Technical University, Zikova 4, 166 36 Prague 6, Czech Republic

¹⁴Dapnia, CEA Saclay, F-91191, Gif-sur-Yvette, France

¹⁵ELTE, Eötvös Loránd University, H-1117 Budapest, Pázmány P. s. 1/A, Hungary

¹⁶Ewha Womans University, Seoul 120-750, Korea

¹⁷Florida Institute of Technology, Melbourne, Florida 32901, USA

¹⁸Florida State University, Tallahassee, Florida 32306, USA

¹⁹Georgia State University, Atlanta, Georgia 30303, USA

²⁰Hiroshima University, Kagamiyama, Higashi-Hiroshima 739-8526, Japan

²¹IHEP Protvino, State Research Center of Russian Federation, Institute for High Energy Physics, Protvino, 142281, Russia

²²University of Illinois at Urbana-Champaign, Urbana, Illinois 61801, USA

²³Institute for Nuclear Research of the Russian Academy of Sciences, prospekt 60-letiya Oktyabrya 7a, Moscow 117312, Russia

²⁴Institute of Physics, Academy of Sciences of the Czech Republic, Na Slovance 2, 182 21 Prague 8, Czech Republic

²⁵Iowa State University, Ames, Iowa 50011, USA

²⁶Joint Institute for Nuclear Research, 141980 Dubna, Moscow Region, Russia

²⁷Helsinki Institute of Physics and University of Jyväskylä, P.O.Box 35, FI-40014 Jyväskylä, Finland

²⁸High Energy Accelerator Research Organization, KEK, Tsukuba, Ibaraki 305-0801, Japan

²⁹KFKI Research Institute for Particle and Nuclear Physics of the Hungarian Academy of Sciences (MTA KFKI RMKI),
H-1525 Budapest 114, POBox 49, Budapest, Hungary

³⁰Korea University, Seoul, 136-701, Korea

³¹Russian Research Center "Kurchatov Institute," Moscow, 123098 Russia

³²Kyoto University, Kyoto 606-8502, Japan

³³Laboratoire Leprince-Ringuet, Ecole Polytechnique, CNRS-IN2P3, Route de Saclay, F-91128, Palaiseau, France

³⁴Lawrence Livermore National Laboratory, Livermore, California 94550, USA

³⁵Los Alamos National Laboratory, Los Alamos, New Mexico 87545, USA

³⁶LPC, Université Blaise Pascal, CNRS-IN2P3, Clermont-Fd, 63177 Aubiere Cedex, France

³⁷Department of Physics, Lund University, Box 118, SE-221 00 Lund, Sweden

³⁸University of Maryland, College Park, Maryland 20742, USA

³⁹Department of Physics, University of Massachusetts, Amherst, Massachusetts 01003-9337, USA

⁴⁰Institut für Kernphysik, University of Muenster, D-48149 Muenster, Germany

⁴¹Muhlenberg College, Allentown, Pennsylvania 18104-5586, USA

⁴²Myongji University, Yongin, Kyonggido 449-728, Korea

⁴³Nagasaki Institute of Applied Science, Nagasaki-shi, Nagasaki 851-0193, Japan

⁴⁴University of New Mexico, Albuquerque, New Mexico 87131, USA

⁴⁵New Mexico State University, Las Cruces, New Mexico 88003, USA

⁴⁶Oak Ridge National Laboratory, Oak Ridge, Tennessee 37831, USA

⁴⁷IPN-Orsay, Université Paris Sud, CNRS-IN2P3, BP1, F-91406, Orsay, France

⁴⁸Peking University, Beijing, People's Republic of China

⁴⁹PNPI, Petersburg Nuclear Physics Institute, Gatchina, Leningrad region, 188300, Russia

⁵⁰RIKEN Nishina Center for Accelerator-Based Science, Wako, Saitama 351-0198, Japan

⁵¹RIKEN BNL Research Center, Brookhaven National Laboratory, Upton, New York 11973-5000, USA

⁵²Physics Department, Rikkyo University, 3-34-1 Nishi-Ikebukuro, Toshima, Tokyo 171-8501, Japan

⁵³Saint Petersburg State Polytechnic University, St. Petersburg, 195251 Russia

⁵⁴Instituto de Física, Universidade de São Paulo, Caixa Postal 66318, São Paulo CEP05315-970, Brazil

⁵⁵*Chemistry Department, Stony Brook University, SUNY, Stony Brook, New York 11794-3400, USA*⁵⁶*Department of Physics and Astronomy, Stony Brook University, SUNY, Stony Brook, New York 11794-3400, USA*⁵⁷*University of Tennessee, Knoxville, Tennessee 37996, USA*⁵⁸*Department of Physics, Tokyo Institute of Technology, Oh-okayama, Meguro, Tokyo 152-8551, Japan*⁵⁹*Institute of Physics, University of Tsukuba, Tsukuba, Ibaraki 305, Japan*⁶⁰*Vanderbilt University, Nashville, Tennessee 37235, USA*⁶¹*Advanced Research Institute for Science and Engineering, Waseda University, 17 Kikui-cho, Shinjuku-ku, Tokyo 162-0044, Japan*⁶²*Weizmann Institute, Rehovot 76100, Israel*⁶³*Yonsei University, IPAP, Seoul 120-749, Korea*

(Received 2 June 2011; published 18 October 2011)

Back-to-back hadron pair yields in $d + \text{Au}$ and $p + p$ collisions at $\sqrt{s_{NN}} = 200$ GeV were measured with the PHENIX detector at the Relativistic Heavy Ion Collider. Rapidity separated hadron pairs were detected with the trigger hadron at pseudorapidity $|\eta| < 0.35$ and the associated hadron at forward rapidity (deuteron direction, $3.0 < \eta < 3.8$). Pairs were also detected with both hadrons measured at forward rapidity; in this case, the yield of back-to-back hadron pairs in $d + \text{Au}$ collisions with small impact parameters is observed to be suppressed by a factor of 10 relative to $p + p$ collisions. The kinematics of these pairs is expected to probe partons in the Au nucleus with a low fraction x of the nucleon momenta, where the gluon densities rise sharply. The observed suppression as a function of nuclear thickness, p_T , and η points to cold nuclear matter effects arising at high parton densities.

DOI: 10.1103/PhysRevLett.107.172301

PACS numbers: 25.75.Dw

Nuclear effects on quark and gluon densities of nucleons bound in nuclei can be studied in collisions of deuteron and gold nuclei at the Relativistic Heavy Ion Collider. At $\sqrt{s_{NN}} = 200$ GeV, the hadron yields in the forward-rapidity (deuteron-going) direction were observed to be suppressed for $d + \text{Au}$ collisions relative to $p + p$ collisions [1–3]. However, the mechanism for the suppression was not firmly established and may indicate novel QCD effects in nuclei. Competing theoretical approaches include initial state energy loss [4,5], parton recombination [6], shadowing effects [7,8], and gluon saturation [9].

Back-to-back dijet yields were proposed as an additional observable to distinguish better between competing mechanisms. The color glass condensate (CGC) framework [10] predicts that quarks and gluons scattering at forward angles (large rapidity) will interact coherently off gluons at low x in the gold nucleus. As a result, the rate of observed recoiling jets is expected to be suppressed in $d + \text{Au}$ collisions compared to $p + p$, and angular broadening of the back-to-back correlation of jets is predicted [11,12]. Dihadron correlation measurements were used [13,14] successfully in $d + \text{Au}$ collisions to select dijet production based on the back-to-back peak at $\Delta\phi = \pi$ between trigger hadrons and their associated hadrons. Dihadron correlation measurements with varying kinematic constraints (transverse momentum p_T and rapidity) probe different x ranges in the nucleus. In particular, measurements at forward rapidity are thought to probe small x values in the Au nucleus.

In this Letter, we report results on the suppression in $d + \text{Au}$ relative to $p + p$ collisions of inclusive π^0 's and back-to-back cluster- π^0 pairs in the forward-rapidity region and for back-to-back π^0 - π^0 or hadron- π^0 pairs separated in rapidity. The data were obtained from $p + p$

and $d + \text{Au}$ runs in 2008 with the PHENIX detector and include a new electromagnetic calorimeter, the muon piston calorimeter (MPC), with an acceptance of $3.0 < \eta < 3.8$ in pseudorapidity and $0 < \phi < 2\pi$. The clusters are reconstructed from the energy deposit of photons in individual MPC towers. The MPC comprises 220 PbWO_4 towers of $20.2X_0$ depth, with lateral dimensions of $2.2 \times 2.2 \text{ cm}^2$, and is located 220 cm along the beam axis from the nominal interaction point.

The $d + \text{Au}$ sample is separated into four centrality classes—0–20% (most central), 20–40%, 40–60%, and 60–88% (most peripheral)—based on charge deposited in the backward (gold direction) beam-beam counter ($3.0 < -\eta < 3.9$). We determine the average number of binary collisions $\langle N_{\text{coll}} \rangle$ from a Glauber model [3] and a simulation of the beam-beam counter; $\langle N_{\text{coll}} \rangle$ values are 15.1 ± 1.0 , 10.2 ± 0.70 , 6.6 ± 0.44 , and 3.2 ± 0.19 , respectively.

The charged hadron (h^\pm) and π^0 analysis in the mid-rapidity region $|\eta| < 0.35$ is identical to that for previous measurements by PHENIX [15,16]. For the analysis in the forward-rapidity region, a fiducial cut is applied, ensuring that clusters are fully reconstructed within the MPC acceptance. Photon candidates are identified in the MPC by comparing cluster candidates to the expected shower profile for photons. The shower profile for photons is determined from the PHENIX GEANT3 [17] based detector simulation, PISA, which was tuned to reproduce MPC test beam data. For the pair analyses reported here, the associated particles in the MPC are π^0 's, which are identified by reconstructing the mass of their decay photon pairs. The π^0 yield is obtained after subtraction of the combinatoric background of uncorrelated photon pairs. The shape of the background was determined from $p + p$ PYTHIA 6.4 [18] and $d + \text{Au}$ HIJING [19] events that are

subsequently processed through PISA. The p_T -dependent systematic uncertainty on the associated π^0 yield extraction procedure is estimated to be 2–5% for $p + p$ and $d + Au$.

The closeness of the MPC to the collision vertex and the high energy of particles emitted in the forward direction make it difficult to reconstruct photon pairs from π^0 decays at high p_T . For example, at $p_T = 1$ GeV/ c , approximately 30% of the photon cluster pairs are merged and cannot be reconstructed separately in the MPC. To extend the p_T range and the pair yield, single electromagnetic clusters are used as trigger particles to construct cluster- π^0 dihadron pairs in the MPC. These trigger clusters are treated assuming that they are all π^0 's. However, PYTHIA studies indicate that $\geq 80\%$ of these trigger clusters are from π^0 's, with the rest being dominantly single photons from asymmetric decays of η mesons or direct photons; thus, according to these studies, a relatively small contamination remains. The cluster energy was corrected to the true π^0 energy to account for the merging effects of the two photons from π^0 decay. These corrections were determined by embedding Monte Carlo generated π^0 's into real data, as well as from PYTHIA tuned to match the data.

Figure 1 shows the azimuthal angle correlations between midrapidity and forward-rapidity π^0 pairs, per π^0 trigger detected at midrapidity, in $p + p$, peripheral $d + Au$, and central $d + Au$ collisions for varying trigger π^0 p_T . Figure 2 shows the same correlations for trigger clusters where the cluster- π^0 pairs are both detected at forward rapidity. The constant pedestal, b_0 , was subtracted from the correlation function. The correlations were corrected for the forward π^0 detection efficiency and for the combinatoric background beneath the π^0 peaks in the photon-pair invariant mass spectra. This background is determined by measurement of the azimuthal correlations for photon-pair mass selections adjacent to the π^0 mass window and from

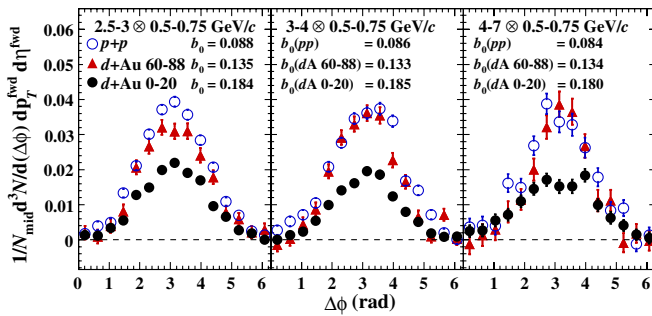


FIG. 1 (color online). Pedestal-subtracted π^0 - π^0 per-trigger correlation functions for, as indicated, $p + p$, $d + Au$ peripheral (60–88% centrality), and $d + Au$ central (0–20% centrality) collisions at $\sqrt{s_{NN}} = 200$ GeV; the associated π^0 's of $p_T = 0.5$ – 0.75 GeV/ c are measured at forward rapidity ($3.0 < \eta < 3.8$), and the triggered π^0 's are measured at midrapidity ($|\eta| < 0.35$) for the indicated p_T ranges. The subtracted pedestal values, b_0 , are also indicated.

studies of simulated jet events from PYTHIA events processed through PISA.

For the midrapidity/forward-rapidity correlations (Fig. 1), due to the large pseudorapidity gap of $\Delta\eta \sim 3.3$ between the hadrons, only an away-side peak ($\Delta\phi = \pi$) is seen. For the forward-forward correlations, a near-side peak ($\Delta\phi = 0$) is also present (see Fig. 2). The yields and widths of the correlated pairs are extracted by fits to an away-side Gaussian signal shape plus a constant background (b_0). The fit to the forward-forward correlations has an additional Gaussian signal for the near-side peak. The pedestal is determined from a fit in the midrapidity/forward-rapidity correlations and is consistent with the pedestal level found based on the assumption that the signal yield is 0 at the minimum of the correlation function—zero yield at minimum (ZYAM) [20]. In the forward-forward correlations, the ZYAM pedestal is used in the yield extraction. Additional systematic uncertainties of up to 30% (not shown in Fig. 2) are ascribed to the near-side peak due to corrections for resonance decays that contaminate the jet signal and due to the acceptance loss around the trigger particle of $\Delta\phi \times \Delta\eta \approx 0.5 \times 0.5$ rad, resulting from the minimum separation cut of one tower between cluster peaks in the MPC. The acceptance loss gives rise to the decrease observed for the near-side peak.

Figures 1 and 2 show that the away-side peak for $d + Au$ central collisions is suppressed compared to $p + p$ collisions and peripheral $d + Au$ collisions. This effect is large for the midrapidity/forward-rapidity correlations (Fig. 1) and becomes even larger when both particles are required to be in the forward-rapidity region (Fig. 2).

For the midrapidity/forward-rapidity correlations, within their large uncertainties, the Gaussian widths of the away-side correlation peak remain the same between $p + p$ and central $d + Au$, and the broadening predicted in

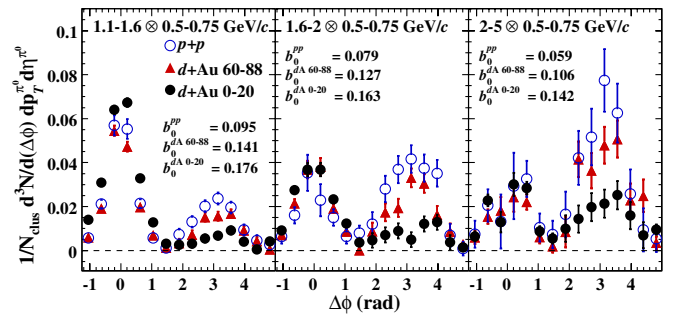


FIG. 2 (color online). Pedestal-subtracted cluster- π^0 per-trigger correlation functions measured at forward rapidity ($3.0 < \eta < 3.8$) for, as indicated, $p + p$, $d + Au$ peripheral (60–88% centrality), and $d + Au$ central (0–20% centrality) collisions at $\sqrt{s_{NN}} = 200$ GeV; the correlation functions are for associated π^0 's of $p_T = 0.5$ – 0.75 GeV/ c and trigger clusters over the indicated p_T ranges. Systematic uncertainties of up to 30% on the near side ($|\Delta\phi| < 0.5$) are not shown. The subtracted pedestal values, b_0 , are also indicated.

the CGC framework in Ref. [11] is not observed. For example, in $d + \text{Au}$ central collisions, $\sigma = 0.93 \pm 0.09^{\text{stat}} \pm 0.139^{\text{syst}}$ for $p_T^{\text{fwd}} = 1.25 \text{ GeV}/c$ and trigger particle momentum $2.5 < p_T^t < 3.0 \text{ GeV}/c$, while $\sigma = 0.97 \pm 0.07^{\text{stat}} \pm 0.08^{\text{syst}}$ for $p + p$ collisions. For the forward-forward correlations, the measurement does not discern whether there is appreciable broadening between $d + \text{Au}$ and $p + p$ collisions, as the ZYAM pedestal determination can bias the widths to smaller values.

The observed suppression is quantified by studying the relative yield, J_{dA} [21], of correlated back-to-back hadron pairs in $d + \text{Au}$ collisions compared to $p + p$ collisions scaled with $\langle N_{\text{coll}} \rangle$,

$$J_{dA} = I_{dA} \times R_{dA}^t = \frac{1}{\langle N_{\text{coll}} \rangle} \frac{\sigma_{dA}^{\text{pair}} / \sigma_{dA}}{\sigma_{pp}^{\text{pair}} / \sigma_{pp}}, \quad (1)$$

where $R_{dA}^t = (1/\langle N_{\text{coll}} \rangle)(\sigma_{dA}^t / \sigma_{dA}) / (\sigma_{pp}^t / \sigma_{pp})$ is the usual nuclear modification factor for trigger particles t , and σ , σ^t , and σ^{pair} are the cross sections (or normalized yields) for the full event selection, trigger particle event selection, and dihadron pair event selection. I_{dA} is the ratio of conditional hadron yields, CY , for $d + \text{Au}$ and $p + p$ collisions:

$$CY = \frac{\int d(\Delta\phi) [dN/d(\Delta\phi) - b_0]}{N^t \times \epsilon^a \times \Delta\eta^a \times \Delta p_T^a}, \quad (2)$$

with the acceptance corrected dihadron correlation function $dN/d(\Delta\phi)$, the number of trigger particles N^t , the

detection efficiency for the associated particle ϵ^a , and the level of the uncorrelated pedestal in the correlation functions b_0 . The integral is taken over the Gaussian fit of the away-side peak. The J_{dA} uncertainties include a systematic uncertainty from the ZYAM pedestal subtraction. In determining this uncertainty, it was assumed that changes between $d + \text{Au}$ and $p + p$ in the Gaussian away-side width remain below a factor two. This upper limit is based on the small observed changes in width in the midrapidity/forward-rapidity correlations and the correlations studied previously with the PHENIX muon spectrometers [14]. The J_{dA} is calculated from the measured I_{dA} and R_{dA}^t for the forward-rapidity trigger correlations with the new π^0 $R_{dAu} = R_{dAu}^t$ determined in the MPC. For the midrapidity trigger correlations, published values for R_{dA} from the 2003 RHIC run [15,16] were used.

Figure 3 presents J_{dA} versus $\langle N_{\text{coll}} \rangle$ for forward-rapidity π^0 's paired with midrapidity hadrons and π^0 's and for π^0 's and clusters paired at forward rapidity. The J_{dA} decreases with an increasing number of binary collisions, $\langle N_{\text{coll}} \rangle$, or equivalently with increasing nuclear thickness. The suppression also increases with decreasing particle p_T and is significantly larger for forward-forward hadron pairs than for midrapidity/forward-rapidity pairs. The observed suppression of J_{dA} versus nuclear thickness, p_T , and η points to large cold nuclear matter effects arising at high parton densities in the nucleus probed by the deuteron, consistent with predictions from CGC [12]. This trend is seen more clearly in Fig. 4, where J_{dA} is plotted versus

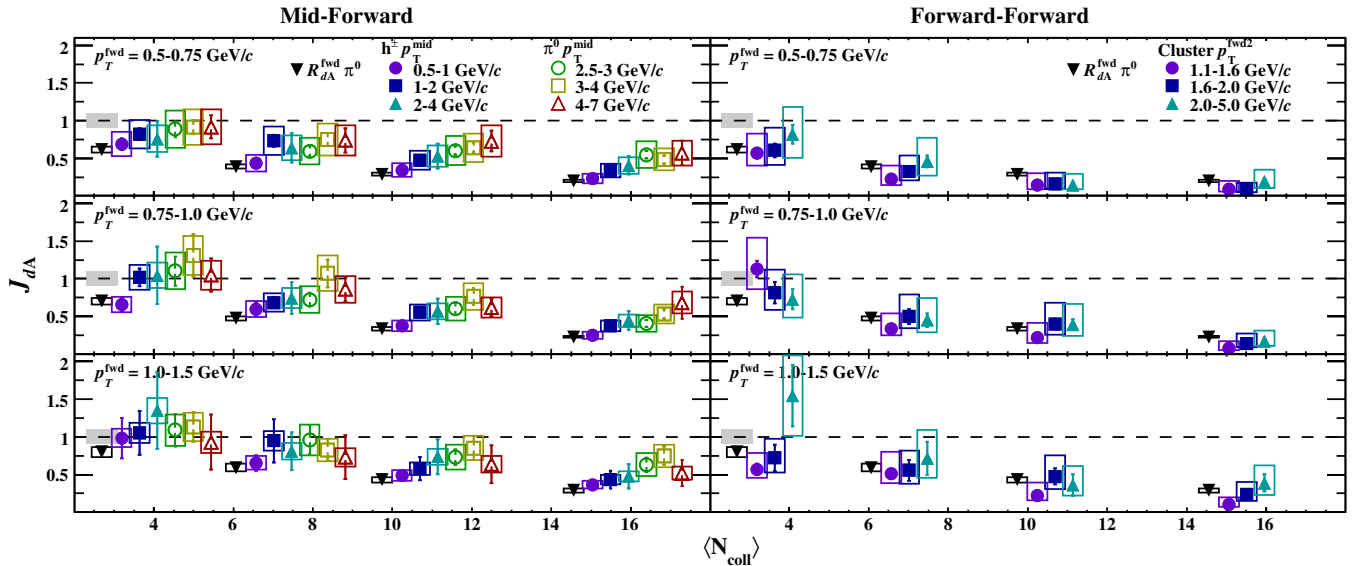


FIG. 3 (color online). Relative yield J_{dA} versus $\langle N_{\text{coll}} \rangle$ for forward-rapidity ($3.0 < \eta < 3.8$) π^0 's paired with (left) midrapidity ($|\eta| < 0.35$) hadrons and π^0 's and (right) forward-rapidity ($3.0 < \eta < 3.8$) cluster- π^0 pairs for the indicated combinations of p_T ranges. Also plotted as inverted solid triangles are the values of the forward π^0 R_{dA} . Around each data point, the vertical bars indicate statistical uncertainties, and the open boxes indicate point-to-point systematic uncertainties. The gray bar at the left in each panel represents a global systematic scale uncertainty of 9.7%. Additional centrality dependent systematic uncertainties of 7.5%, 5.1%, 4.1%, and 4.8% for the peripheral to central bins, respectively, are not shown. The $\langle N_{\text{coll}} \rangle$ values within a centrality selection are offset from their actual values for visual clarity (see text for actual $\langle N_{\text{coll}} \rangle$ values).

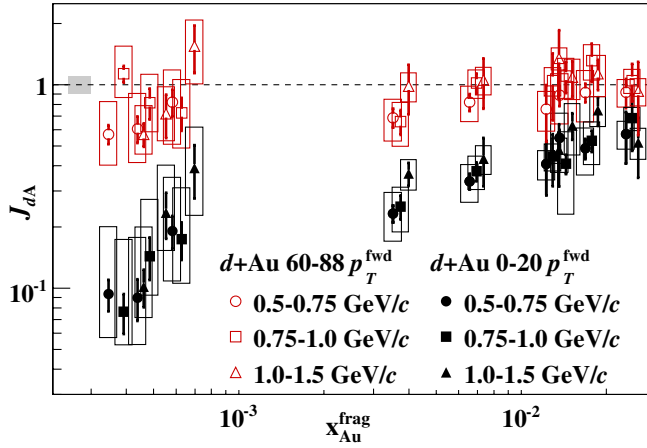


FIG. 4 (color online). J_{dA} versus x_{Au}^{frag} for peripheral (60–88%) and central (0–20%) $d + Au$ collisions at $\sqrt{s_{NN}} = 200$ GeV. The statistical error bars and systematic uncertainty boxes are the same as in Fig. 3. Above $x_{Au}^{\text{frag}} > 10^{-3}$, some data points were offset from their true x_{Au}^{frag} to avoid overlap. The leftmost point in each group of three is at the correct x_{Au}^{frag} .

$x_{Au}^{\text{frag}} = (\langle p_{T1} \rangle e^{-\langle \eta_1 \rangle} + \langle p_{T2} \rangle e^{-\langle \eta_2 \rangle}) / \sqrt{s_{NN}}$ for all pair selections in η and p_T . In the case of $2 \rightarrow 2$ parton scattering, where two final state hadrons carry the full parton energy, $z = 1$, the variable x_{Au}^{frag} would be equal to $\langle x_{Au} \rangle$, which is the average momentum fraction of the struck parton in the Au nucleus.

Because the fragmentation hadrons on average carry a momentum fraction $\langle z \rangle < 1$, x_{Au}^{frag} will be smaller than $\langle x_{Au} \rangle$. Based on previous studies by PHENIX at midrapidity, the mean fragmentation $\langle z \rangle$ is expected to be between 0.5–0.75 [22]. In general, the theoretical extraction of x_{Au} from the measured p_T and η will differ from the leading-order QCD picture of $2 \rightarrow 2$ processes used above. Also, at modest p_T 's, the interpretation of the measured correlation functions as high energy $2 \rightarrow 2$ parton scattering accessing low x may be limited by contributions from processes with small momentum transfer Q^2 . Future theoretical analysis will be necessary to evaluate these and other contributions from different nuclear effects [4–10] on the observed large suppression in J_{dA} . These analyses could additionally be complicated by the presence of hadron pairs originating from multiparton interactions [23] that might not probe gluon structure at low x_{Au} .

In summary, measurements of the inclusive π^0 yield at forward rapidity, of the back-to-back correlated yield of cluster- π^0 pairs in the forward-rapidity region, and of the correlated yield of forward-rapidity π^0 's with midrapidity π^0 's or hadrons in $p + p$ and $d + Au$ collisions at $\sqrt{s_{NN}} = 200$ GeV were presented. The correlated yields of back-to-back pairs were analyzed for various kinematic selections in p_T and rapidity. The forward-central pair measurements show no increase in the azimuthal angular correlation width within experimental uncertainties. The correlated

yield of back-to-back pairs in $d + Au$ collisions is observed to be substantially suppressed relative to $p + p$ collisions with a suppression that is observed to increase with decreasing impact parameter selection and for pairs probing more forward rapidities.

We thank the staff of the Collider-Accelerator and Physics Departments at Brookhaven National Laboratory and the staff of the other PHENIX participating institutions for their vital contributions. We acknowledge support from the Office of Nuclear Physics in the Office of Science of the Department of Energy, the National Science Foundation, Abilene Christian University Research Council, Research Foundation of SUNY, and Dean of the College of Arts and Sciences, Vanderbilt University (U.S.A.); Ministry of Education, Culture, Sports, Science, and Technology and the Japan Society for the Promotion of Science (Japan); Conselho Nacional de Desenvolvimento Científico e Tecnológico and Fundação de Amparo à Pesquisa do Estado de São Paulo (Brazil); Natural Science Foundation of China (P. R. China); Ministry of Education, Youth, and Sports (Czech Republic); Centre National de la Recherche Scientifique, Commissariat à l'Énergie Atomique, and Institut National de Physique Nucléaire et de Physique des Particules (France); Ministry of Industry, Science and Technologies, Bundesministerium für Bildung und Forschung, Deutscher Akademischer Austausch Dienst, and Alexander von Humboldt Stiftung (Germany); Hungarian National Science Fund, OTKA (Hungary); Department of Atomic Energy and Department of Science and Technology (India); Israel Science Foundation (Israel); National Research Foundation and WCU Program of the Ministry of Education, Science, and Technology (Korea); Ministry of Education and Science, Russian Academy of Sciences, and Federal Agency of Atomic Energy (Russia); VR and the Wallenberg Foundation (Sweden); the U.S. Civilian Research and Development Foundation for the Independent States of the Former Soviet Union, the U.S.-Hungarian Fulbright Foundation for Educational Exchange, and the U.S.-Israel Binational Science Foundation.

*Deceased

†PHENIX spokesperson.

jacak@skipper.physics.sunysb.edu

- [1] I. Arsene *et al.* (BRAHMS Collaboration), *Phys. Rev. Lett.* **93**, 242303 (2004).
- [2] J. Adams *et al.* (STAR Collaboration), *Phys. Rev. Lett.* **97**, 152302 (2006).
- [3] S. S. Adler *et al.* (PHENIX Collaboration), *Phys. Rev. Lett.* **94**, 082302 (2005).
- [4] I. Vitev, *Phys. Rev. C* **75**, 064906 (2007).
- [5] L. Frankfurt and M. Strikman, *Phys. Lett. B* **645**, 412 (2007).
- [6] R. C. Hwa, C. B. Yang, and R. J. Fries, *Phys. Rev. C* **71**, 024902 (2005).

- [7] V. Guzey, M. Strikman, and W. Vogelsang, *Phys. Lett. B* **603**, 173 (2004).
- [8] J. Qiu and I. Vitev, *Phys. Lett. B* **632**, 507 (2006).
- [9] L. Gribov, E. Levin, and M. Ryskin, *Phys. Rep.* **100**, 1 (1983).
- [10] L. McLerran and R. Venugopalan, *Phys. Rev. D* **49**, 3352 (1994).
- [11] D. Kharzeev, E. Levin, and L. McLerran, *Nucl. Phys.* **A748**, 627 (2005).
- [12] C. Marquet, *Nucl. Phys.* **A796**, 41 (2007).
- [13] S. S. Adler *et al.* (PHENIX Collaboration), *Phys. Rev. C* **73**, 054903 (2006).
- [14] S. S. Adler *et al.* (PHENIX Collaboration), *Phys. Rev. Lett.* **96**, 222301 (2006).
- [15] S. S. Adler *et al.* (PHENIX Collaboration), *Phys. Rev. C* **77**, 014905 (2008).
- [16] S. S. Adler *et al.* (PHENIX Collaboration), *Phys. Rev. Lett.* **98**, 172302 (2007).
- [17] R. Brun *et al.*, Report No. CERN-DD-EE-84-1 (1987).
- [18] T. Sjostrand, S. Mrenna, and P.Z. Skands, *J. High Energy Phys.* **05** (2006) 026.
- [19] X.-N. Wang and M. Gyulassy, *Phys. Rev. D* **44**, 3501 (1991).
- [20] N.N. Ajitanand *et al.*, *Phys. Rev. C* **72**, 011902 (2005).
- [21] A. Adare *et al.* (PHENIX Collaboration), *Phys. Rev. C* **78**, 014901 (2008).
- [22] S. S. Adler *et al.* (PHENIX Collaboration), *Phys. Rev. D* **74**, 072002 (2006).
- [23] M. Strikman and W. Vogelsang, *Phys. Rev. D* **83**, 034029 (2011).